

Differential Protein Expression at the Stage of Neural Tube Closure in the Mouse Embryo*

Received for publication, April 15, 2002, and in revised form, August 8, 2002
Published, JBC Papers in Press, August 27, 2002, DOI 10.1074/jbc.M203607200

Nicholas D. E. Greene^{‡§}, Kit-Yi Leung[¶], Robin Wait^{**}, Shajna Begum^{**}, Michael J. Dunn^{¶‡‡},
and Andrew J. Copp[‡]

From the [‡]Neural Development Unit, Institute of Child Health, University College London, London WC1N 1EH, United Kingdom, the [¶]National Heart & Lung Institute, Imperial College School of Medicine, Heart Science Centre, Harefield Hospital, Middlesex UB9 6JH, United Kingdom, and the ^{**}Kennedy Institute of Rheumatology Division, Faculty of Medicine, Imperial College School of Science, Technology and Medicine, Hammersmith, London W6 8LH, United Kingdom

Analysis of the protein complement of a biological system through proteomics provides the opportunity to directly monitor the functional readout of gene expression. In this study, proteomics was applied to the mouse embryo to investigate the molecular events underlying the processes occurring at the stage of neural tube closure. Protein profiles of embryos between embryonic days 8.5 and 10.5 exhibited a number of stage-specific changes. Identification of developmentally regulated proteins by mass spectrometry revealed several groups of functionally related proteins including circulatory, cytoskeletal, and stress proteins. Additional proteins of unknown function were identified, such as Copine 1 and PICOT, whose developmental regulation was previously unsuspected.

As the mouse genomic sequencing effort approaches completion, a major challenge in developmental biology is to understand the role of each of the encoded proteins in the processes of embryogenesis. Alterations in gene expression underlying a particular developmental event can be investigated either by selecting individual genes or by global screening approaches that do not require preselection of the genes to be analyzed.

In general, mRNA-based screens depend on differential expression techniques such as subtractive hybridization, cDNA microarrays or oligonucleotide chips. Although undoubtedly powerful, these techniques are not necessarily comprehensive in the context of gene expression at the protein level. Interpretation may be hindered by poor correlation between mRNA and protein abundance because of post-transcriptional control. In yeast, abundance of some proteins varies by as much as 20-fold at apparently equivalent mRNA concentrations (1). In mammalian systems, similarly imprecise correlation has been described for proteins in rat bladder (2, 3) and human liver (4). A

further limitation of mRNA-based approaches is the inability to detect proteolytic processing or post-translational modifications that may determine protein activity.

An alternative approach is direct screening of the protein profile, or proteome, of a sample using two-dimensional polyacrylamide gel electrophoresis and mass spectrometry (MS)¹ to separate and identify proteins (5). Detection of post-translational modifications provides a further level of sensitivity, in terms of regulatory or signaling events. In recent years, technical advances in two-dimensional electrophoresis have increased the utility of this approach as applied to complex protein mixtures. In particular, immobilized pH gradient (IPG) strips provide increased reproducibility, resolution and sample loading capacity compared with synthetic carrier ampholyte approaches used previously (6). A significant step forward in proteomics has also been the development of MS methodology for identification of separated proteins, or even the components of protein mixtures (5).

In mouse embryogenesis the period from embryonic day (E) 8.5 to 10.5 encompasses a series of major developmental events. These include formation of the neural tube, the primordium of the central nervous system, which initiates at the cervical-hindbrain boundary at E8.5 and is completed at E10.5 following closure of the posterior neuropore. Other events during this interval include axial rotation, formation of differentiated somites, and extensive remodeling of the heart with onset of regular contractions. Although many studies have examined the expression and function of specific genes during this period of embryonic development, there have been only a few proteomic studies.

Previously, [³⁵S]methionine labeling was used to examine the pattern of protein synthesis in mouse embryos (7–9). In one study (7), 600–800 protein species were resolved by two-dimensional electrophoresis but only one spot differed in intensity at E8, 9, and 10. This spot was predicted to be a globin protein, based on similar migration by an erythrocyte protein, and differential expression of globins in a concomitant cDNA expression study. Murach *et al.*, (8) detected around 500 proteins on two-dimensional gels of dissected embryos at E7–9, and selected 54 spots or groups of spots for analysis. Among these, 11 spots differed in level in embryonic tissues at E7–9, although the identity of these proteins was not determined. A potential drawback of these studies (7–9) is that embryos were

* This work was supported by the Wellcome Trust (to N. G., A. C., R. W., S. B.), Arthritis Research Campaign (to K. L., R. W., M. D.), Medical Research Council (to R. W., S. B.), and the British Heart Foundation (to M. D.). The costs of publication of this article were defrayed in part by the payment of page charges. This article must therefore be hereby marked "advertisement" in accordance with 18 U.S.C. Section 1734 solely to indicate this fact.

§ To whom correspondence should be addressed: Neural Development Unit, Inst. of Child Health, Guilford St., London, WC1N 1EH United Kingdom. Tel.: 44-2079052230; Fax: 44-2078314366; E-mail: n.greene@ich.ucl.ac.uk.

¶ Present address: Proteome Sciences plc, Institute of Psychiatry, King's College, De Crespigny Park, London SE5 8AF, United Kingdom.

‡‡ Present address: Dept. of Neuroscience, Inst. of Psychiatry, King's College, De Crespigny Park, London, United Kingdom.

¹ The abbreviations used are: MS, mass spectrometry; IPG, immobilized pH gradient; CHAPS, 3-[(3-cholamidopropyl)dimethylammonio]-1-propanesulfonic acid; ESI, electrospray ionization; MALDI, matrix-assisted laser desorption/ionization; AFP, α -fetoprotein.

labeled in tissue culture medium that does not support normal physiological development, the optimal culture medium for organogenesis-stage embryos being rat serum (10). Labeling proteins under non-physiological conditions introduces the potential for spurious results that do not reflect *in vivo* development.

In view of the advances in two-dimensional electrophoresis technology over the past decade, a re-evaluation of the potential application of proteomic methodology to embryological systems seems timely and appropriate. In this study, we used IPG-based two-dimensional electrophoresis followed by silver staining and direct identification of proteins by MS, to monitor changes in the protein profile of mouse embryos over the period E8.5–10.5.

EXPERIMENTAL PROCEDURES

Mouse Embryo Collection—CD1 mice (Charles River) were mated overnight and females checked for copulation plugs the following morning, designated E0.5. At E8.5, E9.5, or E10.5 mice were killed and the uterus explanted into Dulbecco's modified Eagle's medium. Embryos were dissected free of extra-embryonic membranes, washed in phosphate-buffered saline, rinsed in distilled water, and immediately frozen on dry ice. Samples containing pools of four embryos at E8.5, two embryos at E9.5 or single embryos at E10.5, were stored at -70°C . Initial analysis was based on comparison of three independent samples for each stage and a further two samples for each stage were used for confirmation of results (fifteen samples in total).

Two Dimensional Polyacrylamide Gel Electrophoresis—Embryos were resuspended in 200 μl of lysis buffer containing 9.5 M urea, 2% CHAPS, 0.8% pharmalyte pH 3–10, 1% dithiothreitol, with $1\times$ protease inhibitor mixture and phosphatase inhibitor mixture (Sigma) and homogenized by sonication. Protein concentrations were determined as described (11). Analytical gel loadings, for sample comparison, were 100 μg . Preparative gel loadings, for protein identification, were 400 μg . For isoelectric focusing, samples were applied to pH 3–10, 18-cm non-linear IPG strips (Amersham Biosciences) and two-dimensional electrophoresis was performed, using 12% second dimension gels, as described (11).

Protein Visualization and Image Analysis—Analytical and preparative gels were silver stained and scanned as described (11). Protein patterns were analyzed using PDQUEST software (version 6.2, Bio-Rad, Richmond, CA). Qualitative and quantitative comparisons were made between replicate groups, comprising the three gels for each stage. Quantitation is based on the peak intensity and area of Gaussian-fitted spots, allowing more accurate quantitation than summation of pixel intensities. Any differential spots that were not present or absent in all three gels within a replicate group were excluded. To evaluate the potential for spurious differences that are not stage-specific, we also compared replicate groups in which gels were arbitrarily assigned to one of three groups, each containing one gel from each stage. No differences were detected between these groups, suggesting that the differentially represented spots are genuinely stage-specific. Differences that were identified in the initial nine gels were confirmed on a further two gels for each stage.

Mass Spectrometry—In-gel digestion with trypsin and MALDI MS were performed as described (11). Samples were also analyzed by tandem electrospray mass spectrometry (ESI MS/MS). Spectra were recorded using a Q-ToF spectrometer (Micromass, Manchester, UK) interfaced to a Micromass CapLC capillary chromatograph. Samples were dissolved in 0.1% formic acid, and aliquots were injected onto a 300 $\mu\text{m} \times 15\text{ mm}$ Pepmap C₁₈ column (LC Packings, Amsterdam, NL) and eluted with an acetonitrile/0.1% formic acid gradient. Capillary voltage was 3500 V and data-dependent MS/MS acquisitions were performed on precursors with charge states of 2, 3, or 4 over a survey mass range 540–1000. The collision gas was argon, and the collision voltage was 18–45 V depending on the precursor charge state and mass. Proteins were identified by correlation of uninterpreted spectra to entries in SwissProt and TrEMBL using ProteinLynx Global Server (v 1.0, Micromass).

Western Blot Analysis—Pools of embryos (six at E8.5, three at E9.5, and one at E10.5) were homogenized by sonication in 100 μl of dH₂O. Protein content was assayed using the bicinchoninic acid (BCA) protein assay reagent (Pierce). Five micrograms of total protein lysate was resolved on SDS-PAGE, with Rainbow molecular weight markers (Amersham Biosciences), and transferred to Hybond-P (Amersham Biosciences). Blots were incubated with antibodies to calreticulin (1:1000),

α -fetoprotein (AFP) (1:1000), GRP78 (1:500), or β -tubulin (1:500) (all primary antibodies from Santa Cruz Biotechnology, Inc.). Proteins were detected using horseradish peroxidase-conjugated secondary antibodies (DAKO), followed by development with ECL+plus Western blotting Detection System (Amersham Biosciences). Blots were repeated at least three times for each protein.

Semiquantitative RT-PCR—Total RNA was purified from pools of embryos at E8.5 and E10.5 using TRIzol Reagent (Invitrogen Life Technologies). First strand cDNA was generated using the Super-script First-Strand Synthesis System (Invitrogen Life Technologies). One microliter of cDNA was subjected to PCR using gene-specific primers that were designed to cross introns such that any products from amplification of genomic DNA contamination in the sample would be distinguishable. Primer sequences were as follows: HPRT (5'-AAGGACCTCTCGAAGTGTG; 5'-CCTTCTTACAGATAACAATC-TCA), α -fetoprotein (5'-GAACAAGCAGCCATGAAGTG; 5'-CCAGCA-GACACTGATGTCTT), GRP78 (5'-TCATCGGACGCACTTGGAAAT; 5'-TAGTGAGAACCATGGCAGAA), Zeta-Globin (5'-TGAGTGCACTCA-ACTCCAGC; 5'-ACACGCAGGATGTAGGCAT). Samples were amplified for 28 cycles (shown in preliminary tests to be in the linear range), and products were separated on agarose gels. Band intensity was determined using AlphaEase software (v4.0, Alpha Innotech Corporation) and normalized to the band intensity for HPRT. The experiment was repeated in triplicate, and the ratio of abundance at E10.5 compared with E8.5 was calculated.

RESULTS AND DISCUSSION

Despite the proliferation of proteomic studies, the embryo has been somewhat neglected in favor of samples, principally cell lines, in which availability of material is not a limiting factor. Here, we demonstrate the feasibility of functional proteome analysis in the mouse embryo and identify a number of proteins that are developmentally regulated during the period E8.5–10.5. At E8.5, CD1 embryos had 5–7 somites with closure of the neural tube having recently been initiated. Embryos at E9.5 had 17–19 somites, axial rotation was complete, and the neural tube was closed in the cranial region. At E10.5, embryos had 32–33 somites and had completed primary neural tube closure.

Proteome Analysis of Mouse Embryos at E8.5–10.5—In this study, two-dimensional electrophoresis resolved up to 1200 protein spots (Fig. 1), the majority of which are apparently conserved between stages. In previous two-dimensional electrophoresis-based studies of postimplantation mouse embryos, the identity of protein spots of interest was determined in a few cases by indirect methods, such as comigration with known protein samples, that require deduction of possible protein identity (7, 12). This approach is not suitable for novel proteins and not readily applicable to high throughput analysis. Protein elution and chemical sequencing provides the opportunity to obtain peptide sequence but requires relatively large amounts of sample, a major drawback in analysis of embryonic systems. Therefore, we used MS to directly identify embryonic protein species separated by two-dimensional electrophoresis. In addition, we used Western blot analysis to confirm the expression profile of selected proteins identified by two-dimensional electrophoresis (Fig. 2).

Initially, 21 of the most abundant conserved spots, whose staining intensity did not change appreciably between E8.5 and E10.5, were selected for MS analysis. The identity of 18 of these spots was determined, with 16 corresponding to known proteins (Table I). Peptide sequence of the remaining two spots corresponds to known cDNA sequences for which the predicted proteins do not appear in protein databases. These spots provide a reference framework for comparison of the molecular weight and pI observed on gel migration and the theoretical values calculated from amino acid sequence. In most cases the theoretical and observed values were very similar (Table I). Calreticulin (spot 1) ran at a higher molecular weight than predicted, in agreement with Mouse Kidney

FIG. 1. Two-dimensional protein profile for E10.5 CD1 mouse embryo. Proteins were separated on the basis of pI (x-axis) and M_r (molecular mass (kDa) is indicated on y-axis). Numbered spots were identified by MS. Spots 1–18 were present at equal intensity on gels at E8.5–10.5 inclusive, whereas spots 19–42 were expressed at increased levels at E10.5 compared with E8.5.



and Human MRC-5 Fibroblast databases (accessible at biobase.dk/cgi-bin/celis). Western blot analysis of calreticulin (spot 1) and β -tubulin (spot 7) correlated with the observations made using two-dimensional electrophoresis, in that neither of these proteins altered in abundance at the stages examined (Fig. 2).

Protein Profiles Exhibit Stage-specific Changes between E8.5 and 10.5—Comparison of stage-specific groups of gels revealed a number of changes in the protein pattern at successive embryonic days (Fig. 3). At E10.5, a total of 79 spots were increased in intensity by 5-fold or more relative to E8.5. These spots could be broadly grouped into three developmental profiles (Fig. 3). Some spots were up-regulated by E9.5 (profile A) while others were up-regulated at E10.5 compared with both earlier stages examined (profile C). The remainder showed intermediate intensity at E9.5 (profile B). A few spots were present at higher intensity at E10.5 than at E9.5 but not E8.5 (profile D), suggesting that these species were down-regulated between E8.5 and E9.5 and then dramatically up-regulated at E10.5.

A further 22 spots decreased in intensity by 5-fold or more at E10.5 relative to E8.5 (Fig. 3). Among these, 10 showed a relative change of 10-fold or greater. At E9.5, these spots were either present at an intermediate intensity (profile E) or showed a similar degree of down-regulation as at E10.5 (profile F). Five of the spots in this group are located in a chain of increasing pI that includes spot 1, calreticulin (Fig. 4a), which had previously been identified as one of the conserved spots, present at all stages (Table I). The five differentially expressed calreticulin spots are predicted to correspond to different phos-

phorylated forms, although the overall abundance of the calreticulin protein does not change significantly (Fig. 2a). In support of this idea, calreticulin is known to be a substrate for protein kinase C, with at least six potential phosphorylation sites (13). Calreticulin is one of several stress proteins that are differentially regulated at these stages (see below).

Identification of Developmentally Up-regulated Protein Spots—Comparison of E10.5 and E8.5 protein profiles revealed 55 spots that were most dramatically up-regulated at E10.5, exhibiting increases in intensity of 10-fold or more (Fig. 3). Forty of these were located on preparative gels and isolated for MS analysis. Identities were obtained for 24 spots, corresponding to 14 different proteins (Table II). Among the up-regulated proteins, a number could be broadly classified into functionally related groups that may be associated with particular developmental events.

Circulatory Proteins—One of the most abundant up-regulated proteins was identified as zeta globin (Fig. 4b, spot 42). The appearance of this embryonic globin correlates with the establishment, by E9.5, of an extensive embryonic and yolk sac circulation following heart looping and the onset of regular cardiac contractions. There is a corresponding dramatic increase in the number of erythrocytes by E9.5. At this stage the major site of hemopoiesis is the yolk sac (14), although intra-embryonic hemopoiesis begins at around E9.5 (15). In this study the yolk sac was removed, suggesting that the globin detected on two-dimensional gels is principally derived from erythrocytes either in transit or generated within the embryonic vasculature. Interestingly, the detection of increased abundance of an embryonic globin reproduces a previous find-

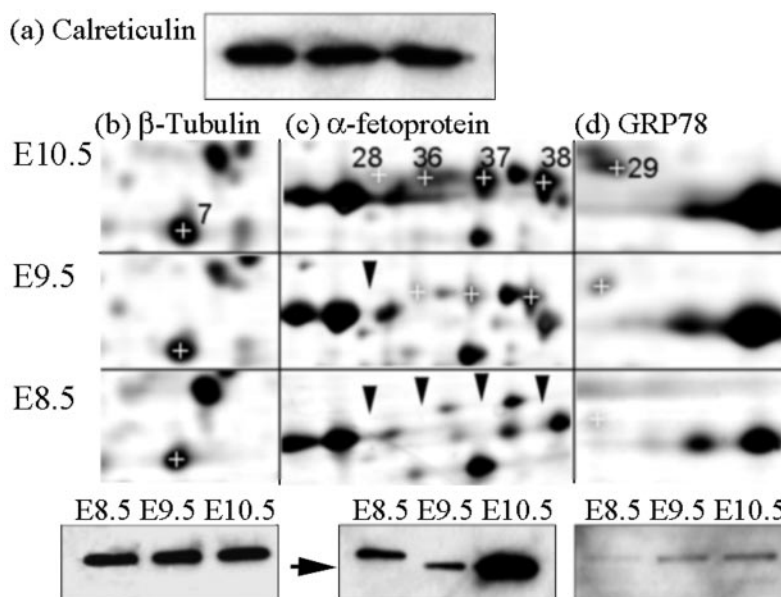


FIG. 2. Stage-specific abundance of individual proteins on two-dimensional electrophoresis correlates with abundance as determined by Western blot. *a*, Western blot of calreticulin (the two-dimensional electrophoresis profile is shown in Fig. 4). *b–d*, representative two-dimensional electrophoresis profiles are shown with the corresponding Western blot beneath for β -tubulin (*b*), α -fetoprotein (*c*), and GRP78 (*d*). On Western blots, band sizes of approximately 55 kDa (*a*), 50 kDa (*b*), 76 kDa (upper band), and 74 kDa (*c*), and 72 kDa (*d*) were as expected. In each case the abundance on two-dimensional electrophoresis and Western blot closely matches. Hence, calreticulin (*a*) and β -tubulin (*b*) are equally abundant at each stage whereas the abundance of GRP78 (*d*) dramatically increases from E8.5–10.5. Similarly, four spots identified as α -fetoprotein (*c*) increase in abundance on two-dimensional electrophoresis from E8.5–10.5 (position of absent spots at E8.5 indicated by arrowheads) corresponding to the increase in intensity of the 74-kDa band on Western blot (arrow in *c*) that is not detected at E8.5.

TABLE I

Identities of abundant unvarying proteins represented on two-dimensional gels of CD1 mouse embryos at E8.5–10.5

Proteins were identified by MS. Spots 2 and 3 match the predicted products of cDNAs for which the corresponding proteins are not present in data bases. Observed M_r/pI values are based on 2-DE migration, and theoretical values are calculated from amino acid sequence. For spot 11 there is no mouse protein in the databases so the closest match, to a known protein of another species, is indicated.

Spot no.	Protein name	Accession number	Observed M_r/pI	Theoretical M_r/pI
1	Calreticulin precursor (Calregulin)	P14211	71.2/4.28	47.98/4.3
2	Translationally controlled transcript (21kDa)	NP_033455	57.9/5.31	19.46/4.8
3	Encoded by day 13 embryo liver cDNA	Q9CY13	50.8/4.8	32.84/4.9
4	60s Acidic Ribosomal protein P0 (L10E)	P14869	37.4/5.29	34.20/6.2
5	Translation initiation factor 3, IF3	gi 12833012	56.4/5.4	37.98/5.5
6	Heat Shock cognate 71kDa protein	P08109	73.1/5.44	70.85/5.4
7	Tubulin Beta-5 chain	P05218	41.1/5.47	49.65/4.8
8	Malate dehydrogenase, cytoplasmic	P14152	39.6/6.05	36.33/6.5
9	T-complex protein 1, Alpha subunit B	P11983	66.2/5.89	60.45/6.1
10	Calcium-independent phospholipase A2	NP_031479	28.7/6.48	24.83/6.3
11	Guanine monophosphate synthase (human)	NP_003866	73.7/6.9	76.72/6.8
12	Peptidyl-prolyl cis-trans isomerase A	P17742	17.8/8.3	17.82/8.3
13	GTP-binding nuclear protein RAN (TC4)	P28746	27.6/7.85	24.41/7.6
14	Transcription factor BTF3	Q64152	20.9/7.93	21.54/9.8
15	Cofilin, non-muscle isoform	P18760	18.7/8.77	18.54/8.5
16	L-lactate dehydrogenase, Mchain	P06151	39.6/8.09	36.50/8.0
17	Guanine nucleotide binding protein, β subunit-like	I49700	35.2/8.11	35.02/8.3
18	Pyruvate kinase, M2 isozyme	P52480	64.8/8.13	57.89/7.7

ing (7), although in that study it was the only protein change detected between E8 and E10.

AFP, the principal serum protein during embryogenesis, was also up-regulated at successive stages. In fact, 5 separate spots (numbers 28, 36, 37, 38, 40) were identified as AFP, 4 of which ran at slightly higher molecular weight than predicted (Table II). As AFP is a glycoprotein, these probably correspond to different post-translationally modified forms. In mice, AFP is initially synthesized in the yolk sac endoderm (16) and then in the liver with mRNA expression being detectable at E9.5 in the hepatic bud and endoderm of the midgut and hindgut (17). Using two-dimensional electrophoresis we confirm that embryonic expression also increases at the protein level from E9.5

(Fig. 2c). Similarly, on Western blots a band of ~74 kDa is present at E9.5 and very abundant at E10.5, but is not detected at E8.5 (Fig. 2c). However, at E8.5 a band of ~76 kDa is detected by the anti-AFP antibody that is not present at either E9.5 or E10.5. The first eighteen amino acids of AFP constitute a putative signal peptide that equates to 2.01 kDa. We suggest, therefore, that the band detected at E8.5 corresponds to the full-length α -fetoprotein precursor polypeptide and that the band detected at E9.5 and E10.5 is the mature protein, following cleavage of the signal peptide. Presumably, the immature polypeptide is not detected at E9.5–10.5 owing to rapid post-translational cleavage. Therefore, Western blotting not only provided confirmation of the increased abundance of species

detected by two-dimensional electrophoresis, but also indicated an additional level of stage-specific regulation suggesting that this is a useful complementary technique.

Cytoskeletal Proteins—Proteins with cytoskeletal function make up another class of differentially expressed proteins. α -Tubulin (spots 22, 23, 26, 33) is a major component of microtubules. Three of the spots ran at slightly higher molecular weight and pI than theoretically predicted, suggesting that they represent post-translationally modified forms, rather than degradation products. F-actin capping protein (spot 24) binds to the ends of actin filaments, preventing filament growth and facilitating regulation of localized actin assembly at the free ends (18). Up-regulation of vimentin (spot 21), a component of intermediate filaments, was also detected at E9.5 and E10.5. This correlates with previous immunofluorescence studies in

which vimentin was first detected at late E8 in the mesoderm, and at E9 in the neural tube with significantly increased levels at E10 (19, 20). Therefore, components of all three principal cytoskeletal systems, comprising the actin microfilament network, tubulin-containing microtubules and the intermediate filament network (21), were up-regulated at E8.5–10.5. Together these data suggest that the processes occurring at this stage require significant synthesis and remodeling of cytoskeletal components.

Stress Proteins—In addition to altered regulation of calreticulin (see previous), we detected up-regulation of heat shock protein 70 (HSP70; spots 34, 35), a closely related glucose-regulated protein, GRP78 (spot 29, Fig. 2), and APG-2 (spot 30), a member of the heat shock protein 110 family not previously reported in the embryo (Table II). In contrast, a heat shock cognate 70 related protein, HSC71, was an abundant species (spot 6), which did not vary in intensity at the stages examined. This correlates with previous studies in which widespread high level expression of HSC71 was detected at E8–17, as well as at pre-implantation stages (22, 23).

In mouse embryos, HSP70 expression has been described, from E8.5 in the extraembryonic tissues and E15.5 in the embryo, although activation of an HSP70-dependent reporter construct occurs at earlier stages (22, 24). The increasing expression of HSP70 at E9.5–10.5 detected in this study may relate to expression of a heat shock transcription factor, HSF2, whose expression peaks at E10 (24). In mouse embryos, expression of GRP78 (spot 29) has been reported in several tissues, notably the heart, neural tube, gut endoderm, and somites (25). These tissues undergo major morphological changes coincident with the up-regulation at E9.5 that we detected by two-dimensional electrophoresis analysis (Table II, Fig. 2). This up-regulation was confirmed by Western blot (Fig. 2).

Heat shock family proteins have been described on the basis of their elevated expression in response to stress. For example, HSP70 is heat inducible while GRP78 and calreticulin respond to endoplasmic reticulum stress such as hypoglycemia or calcium depletion (24, 26). However, despite the abundance of stress proteins detected in this study and the induction by elevated temperature, neurulation stage mouse embryos are highly sensitive to temperature-induced teratogenicity (24). Rather than a stress response, regulation of these proteins

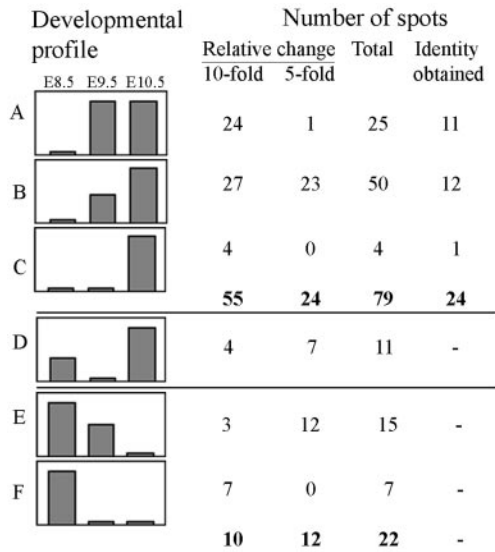


FIG. 3. Histograms indicating representative developmental profiles of spots that are differentially expressed at E8.5–10.5. Bar height represents spot intensity. Relative change indicates a 10-fold quantitative (or qualitative) or 5-fold quantitative difference between bars of minimum and maximum height. Bars of intermediate height indicate spots that do not exhibit a change of this magnitude compared with bars of either maximal or minimal height.

FIG. 4. Differential expression of protein species at E8.5–10.5. Each set (a–d) of nine panels shows a gel region containing one or more differentially expressed spots. The three gels used for initial analysis are shown for each stage. a, spot 1, calreticulin. The chain of spots containing spot 1, contains a greater number of species at E8.5 than E10.5. The white area in spot 1 results from negative staining due to large amounts of protein. b, 42, Hemoglobin zeta chain, absent from E8.5. c, spot 9, T-complex protein 1, α subunit, identified as an abundant conserved spot present on all gels; 39, HMG-CoA synthase, absent from E8.5. d, spots 31, protein kinase STY, and 32, PICOT, both absent at E8.5.

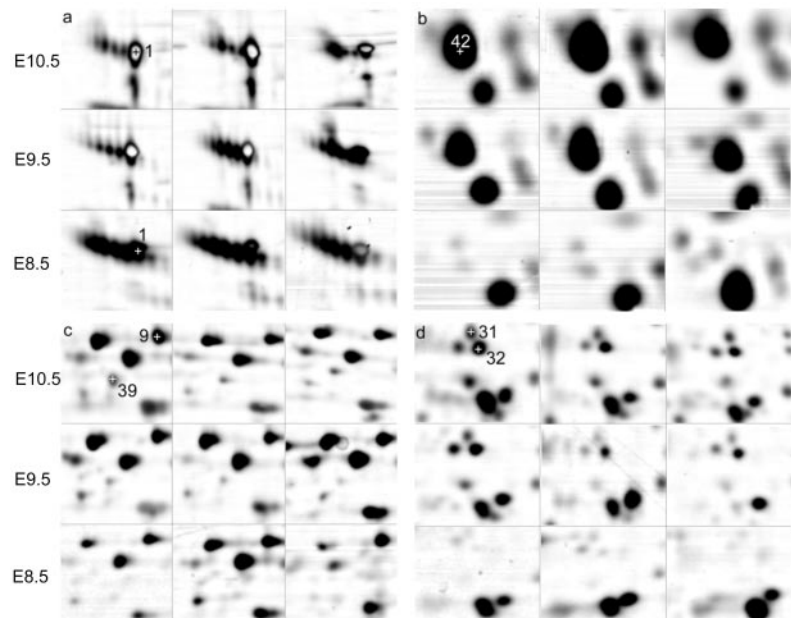


TABLE II
Identities of proteins that are upregulated during the developmental period E8.5–10.5

Spot no.	Protein name	Accession number	Dev. Profile ^a	Observed M_r/pI	Theoretical M_r/pI
19	ATP synthase beta chain, mitochondrial	P56480	A	43.2/5.06	56.36/5.2
20	ATP synthase beta chain, mitochondrial	P56480	A	44/5.03	56.36/5.2
21	Vimentin	P20152	B	63.2/5.25	53.54/5.1
22	Tubulin alpha chain	P02551	A	61.6/5.25	50.12/5.0,
		P05213			50.15/5.0,
		P02516			49.89/5.0
23	Tubulin alpha chain	As above	C	63.5/5.17	As above
24	F-Actin capping protein, alpha-1 subunit	P47753	B	43.4/5.41	32.73/5.5
25	ATP synthase beta chain, mitochondrial	P56480	A	57.9/5.25	56.36/5.2
26	Tubulin alpha chain	As above	A	63.3/5.21	As above
27	Copine 1 (human)	Q99829	B	65.8/5.42	59.04/5.7
28	Alpha-fetoprotein	P02772	B	74.1/5.47	67.34/5.9
29	78 kDa Glucose-regulated protein precursor, GRP78	P20029	A	74.6/5.31	72.40/5.1
30	Heat shock 70-related protein, APG-2	Q61316	A	88.8/5.29	94.06/5.2
31	Protein kinase STY	A39676	B	49.3/5.49	57.08/9.2
32	PKCQ-Interacting protein, PICOT	AAF28842	A	48.2/5.5	37.76/5.6
33	Tubulin alpha chain	As above	B	50.6/5.59	As above
34	Heat shock 70 protein	A45935	A	62.7/5.62	70.84/5.4
35	Heat shock 70 protein	A45935	A	61.8/5.68	70.84/5.4
36	Alpha-fetoprotein	P02772	B	74.2/5.52	67.34/5.9
37	Alpha-fetoprotein	P02772	A	73.8/5.58	67.34/5.9
38	Alpha-fetoprotein	P02772	B	73.5/5.64	67.34/5.9
39	HMG-CoA synthase, cytoplasmic (rat)	P17425	B	62.3/5.82	57.42/5.8
40	Alpha-fetoprotein	P02772	B	64.9/6.92	67.34/5.9
41	Isovaleryl-CoA dehydrogenase, mitochondrial (rat)	P12007	B	49.6/6.91	46.42/8.3
42	Hemoglobin zeta chain	P06467	B	16.1/7.86	16.09/7.7

^a Developmental profile as defined in Fig. 3. For spots 22, 23, 26, and 33, accession numbers and theoretical M_r/pI values are included for tubulin α chain-1, -2, and -6 as, on the basis of the peptide sequences obtained by MS, it was not possible to distinguish between these isotypes.

during neurulation may relate to their function as chaperones that facilitate correct folding and assembly of nascent polypeptide chains in the cytoplasm (HSP70) and the endoplasmic reticulum (GRP78 and calreticulin) (26, 27). Up-regulation of chaperones may therefore be required for function of proteins that regulate or take part in specific events at E9.5–10.5. Similarly, peptidyl-prolyl isomerase, another protein involved in protein folding, was detected as an abundant spot at E8.5–10.5 inclusive (spot 12, Table I).

Coenzyme A-related Enzymes—Isovaleryl-CoA dehydrogenase (spot 41) converts isovaleryl-CoA to 3-methylcrotonyl-CoA, in the leucine degradation pathway (28). This pathway generates acetyl-CoA and acetoacetate, substrates in the ketogenic pathway (29). Acetyl-CoA is also a substrate for another enzyme that was up-regulated, cytoplasmic 3-hydroxy-3-methylglutaryl-CoA (HMG-CoA) synthase (spot 39, Fig. 4c). HMG-CoA synthase catalyzes the condensation of acetoacetyl CoA and acetyl-CoA to form HMG-CoA and free CoA (29). The subsequent conversion of HMG-CoA to mevalonate is the initial step in the cholesterol biosynthetic pathway. An intermediate of this pathway, isopentenyl pyrophosphate, is also the precursor for a wide range of isoprenoid-containing molecules. Coincident up-regulation of these two enzymes suggests that there is an increasing demand for products of the isoprenoid pathway, perhaps cholesterol, at this stage of development.

ATP Synthase—Three up-regulated spots corresponded to ATP synthase β subunit (ATPsyn β) (Spots 19, 20, 25; Table II). ATPsyn β is a key component of the mitochondrial F_0F_1 ATP synthase and, as such, is critical for generation of ATP by oxidative phosphorylation. Although, ubiquitous in mammalian cells, ATPsyn β expression is highly regulated at the transcriptional and translational levels depending on cell type, metabolic requirements, and proliferative state (30). Our data suggest that there is a significant, at least 10-fold, increase in the abundance of ATPsyn β at E8.5–10.5, that may reflect increased demand for ATP as the embryo undergoes a period of rapid growth and morphological change. At this stage the embryo is also making the transition from anaerobic (E8.5) to

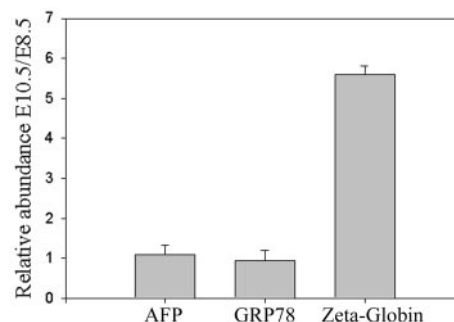


FIG. 5. Relative expression of mRNA at E10.5 and E8.5 for developmentally regulated proteins. The ratio of abundance at E10.5 relative to E8.5 ($E10.5/E8.5$) is plotted (means \pm S.E.). For AFP and GRP78 the mRNA levels are approximately equal (relative ratio of one) whereas there is a marked increase in the expression of zeta-globin at E10.5 compared with E8.5 (relative ratio of six).

aerobic metabolism (E10.5), with a corresponding demand for the proteins involved in oxidative phosphorylation.

Additional Proteins—In some cases, very little is known about the function of proteins that were identified on gels on the basis of differential developmental expression. Copine (spot 27) was initially identified as a calcium-dependent phospholipid-binding protein in *Paramecium* and has homologues in a range of species from plants to mammals, including mouse and human (31). In addition to Ca^{2+} and phospholipid binding domains, the protein has a core domain related to the integrin A domain and has Mg^{2+} and Mn^{2+} binding activity (32). Copine I has been proposed to have a possible role in membrane trafficking or signal transduction. Although present in all major adult organs (32), expression of Copine I has not previously been described in the embryo and a developmental role has not been proposed.

Another up-regulated protein (spot 32) was PICOT (PKC-interacting cousin of thioredoxin) a protein recently isolated owing to its interaction with protein kinase C- θ (PKC θ) (33). The interaction is mediated by an N-terminal thioredoxin homology domain that is followed by two tandem repeats of a

novel conserved domain. Overexpression of PICOT inhibits activation of c-Jun N-terminal kinase by PKC θ suggesting a possible regulatory role (33). PKC θ expression during mouse embryogenesis correlates with sites of hemopoiesis, in the yolk sac blood islands from E9 and the hepatic bud from E10 (34). Neuronal expression is first detected at E10.5. Therefore, the up-regulation of PICOT (Fig. 4d) correlates with the onset of PKC θ expression. However, the incomplete overlap of PICOT and PKC θ localization at the subcellular level and the ability to also interact with PKC ζ , suggest that PICOT may have additional developmental roles (33). STY (spot 31; Fig. 4d) is a dual specificity kinase capable of phosphorylating serine, threonine, and tyrosine residues. A possible function in cell cycle control has been proposed but a specific role in development has not been proposed (35, 36).

Relationship between Protein and mRNA Abundance—As described in the introduction, one of the factors determining the use of a protein-based approach in this study was previous reports showing that mRNA and protein levels may not correlate well (1–4). Therefore, we used semi-quantitative RT-PCR to compare the relative abundance of mRNA for proteins that were shown to be up-regulated between E8.5 and E10.5. In the case of zeta-globin (Fig. 4b, spot 42) there was a significant increase (at least 6-fold) in mRNA abundance between E8.5 and E10.5 (Fig. 5) that correlates with the increase at the protein level. In contrast, the abundance of mRNA for AFP and GRP78 were approximately equal at E8.5 and E10.5 (Fig. 5). In the case of AFP, this is not surprising since although there is a dramatic increase in the abundance of the mature protein at E10.5, the unprocessed protein is present at E8.5 (Fig. 2c). However, for GRP78 the elevated protein abundance at E10.5 does not correlate with a detectable change in mRNA quantity suggesting that there is an additional level of post-transcriptional regulation.

In this study a considerably greater number of proteins was resolved than in previous studies of E8.5 to E10.5 mouse embryos (7–9), probably reflecting improvements in separation methodology. Moreover, use of silver staining gave a global display of the sample, whereas previous analyses of [³⁵S]methionine-labeled proteins was, by necessity, limited to those proteins synthesized during the labeling period (8, 9). The approach taken in this study enabled detection of changes in the abundance of individual protein species and these observations correlated closely with the abundance of the corresponding proteins as determined by Western blot. Moreover, stage-specific regulation of translation (e.g. GRP78) and post-translational modification (e.g. AFP) was observed, which would not have been detected in an mRNA-based study.

Despite improvements in two-dimensional electrophoresis technology the limitation of this technique remains the number of protein spots that are resolved (37). Indeed, we did not detect altered abundance or migration of signaling molecules or transcription factors that regulate several processes at this stage of development, but that are only present at low copy number. For a more comprehensive analysis, additional proteins could be visualized by separation on a series of narrower pH range IPG strips, thereby increasing loading capacity and sensitivity. Study of isolated tissues could also increase abundance of specific proteins. For example, two-dimensional electrophoresis of proteins from the posterior neuropore region enabled identification of transferrin as a

protein taken up during neurulation (12). Future studies will also require preselection of proteins by fractionation into cellular (e.g. nuclear proteins) or functional (e.g. phosphoproteins) components of interest. As an alternative to two-dimensional electrophoresis, such enriched fractions could be analyzed by LC-MS/MS, that has the capability to detect low abundance proteins in complex mixtures (38).

In summary, the application of two-dimensional electrophoresis and MS to embryonic samples provides the opportunity for global analysis of the proteome at specific developmental stages or under different conditions. This may be particularly relevant to the study of systems, including many targeted mutant mice, in which the underlying pathological mechanisms are unknown.

REFERENCES

- Gygi, S. P., Rochon, Y., Franza, B. R., and Aebersold, R. (1999) *Mol. Cell. Biol.* **19**, 1720–1730
- Vizzard, M. A., Wu, K. H., and Jewett, I. T. (2000) *Brain Res. Dev. Brain Res.* **119**, 217–224
- Awad, M. M., and Gruppuso, P. A. (2000) *Cell Growth & Differ.* **11**, 325–334
- Anderson, L., and Seilhamer, J. (1997) *Electrophoresis* **18**, 533–537
- Pandey, A., and Mann, M. (2000) *Nature* **405**, 837–846
- Gorg, A., Obermaier, C., Boguth, G., Harder, A., Scheibe, B., Wildgruber, R., and Weiss, W. (2000) *Electrophoresis* **21**, 1037–1053
- Wilkinson, D. G., Bailes, J. A., Champion, J. E., and McMahon, A. P. (1987) *Development* **99**, 493–500
- Murach, K.-F., Frei, M., Gerhäuser, D., and Illmensee, K. (1990) *J. Cell. Biochem.* **44**, 19–37
- Latham, K. E., Beddington, R. S. P., Solter, D., and Garrels, J. I. (1993) *Mol. Reprod. Dev.* **35**, 140–150
- Cockroft, D. L. (1990) in *Postimplantation Mammalian Embryos: A Practical Approach* (Copp, A. J., and Cockroft, D. L., eds), pp. 15–40, IRL Press, Oxford
- Leung, K. Y., Wait, R., Welson, S. Y., Yan, J. X., Abraham, D. J., Black, C. M., Pearson, J. D., and Dunn, M. J. (2001) *Proteomics* **1**, 787–794
- Copp, A. J., Estibeiro, J. P., Brook, F. A., and Downs, K. M. (1992) *Dev. Biol.* **153**, 312–323
- Rendon-Huerta, E., Mendoza-Hernandez, G., and Robles-Flores, M. (1999) *Biochem. J.* **344 Pt 2**, 469–475
- Kovach, J. S., Marks, P. A., Russell, E. S., and Epler, H. (1967) *J. Mol. Biol.* **25**, 131–142
- De Bruijn, M. F. T. R., Speck, N. A., Peeters, M. C. E., and Dzierzak, E. (2000) *EMBO J.* **19**, 2465–2474
- Dziadek, M. (1978) *J. Embryol. Exp. Morphol.* **46**, 135–146
- Jones, E. A., Clement-Jones, M., James, O. F. W., and Wilson, D. I. (2001) *J. Anat.* **198**, 555–559
- Cooper, J. A., and Schafer, D. A. (2000) *Curr. Opin. Cell Biol.* **12**, 97–103
- Jackson, B. W., Grund, C., Winter, S., Franke, W. W., and Illmensee, K. (1981) *Differentiation* **20**, 203–216
- Houle, J., and Fedoroff, S. (1983) *Brain Res.* **285**, 189–195
- Herrmann, H., and Aebi, U. (2000) *Curr. Opin. Cell Biol.* **12**, 79–90
- Loones, M. T., Rallu, M., Mezger, V., and Morange, M. (1997) *Cell. Mol. Life Sci.* **53**, 179–190
- Hatayama, T., Takigawa, T., Takeuchi, S., and Shiota, K. (1997) *Cell Struct. Funct.* **22**, 517–525
- Walsh, D., Li, Z., Wu, Y., and Nagata, K. (1997) *Cell. Mol. Life Sci.* **53**, 198–211
- Barnes, J. A., and Smoak, I. W. (2000) *Anat. Embryol.* **202**, 67–74
- Lee, A. S. (2001) *Trends Biochem. Sci.* **26**, 504–510
- Agashe, V. R., and Hartl, F. U. (2000) *Semin. Cell Dev. Biol.* **11**, 15–25
- Mohsen, A. W., Anderson, B. D., Volchenbom, S. L., Battaile, K. P., Tiffany, K., Roberts, D., Kim, J. J., and Vockley, J. (1998) *Biochemistry* **37**, 10325–10335
- Hegardt, F. G. (1999) *Biochem. J.* **338**, 569–582
- Poynton, R. O., and McEwen, J. E. (1996) *Annu. Rev. Biochem.* **65**, 563–607
- Creutz, C. E., Tomsig, J. L., Snyder, S. L., Gautier, M. C., Skouri, F., Beisson, J., and Cohen, J. (1998) *J. Biol. Chem.* **273**, 1393–1402
- Tomsig, J. L., and Creutz, C. E. (2000) *Biochemistry* **39**, 16163–16175
- Witte, S., Villalba, M., Bi, K., Liu, Y., Isakov, N., and Altman, A. (2000) *J. Biol. Chem.* **275**, 1902–1909
- Wilda, M., Ghaffari-Tabrizi, N., Reisert, I., Utermann, G., Baier, G., and Hameister, H. (2001) *Mech. Dev.* **103**, 197–200
- Ben-David, Y., Letwin, K., Tannock, L., Bernstein, A., and Pawson, T. (1991) *EMBO J.* **10**, 317–325
- Duncan, P. I., Howell, B. W., Marius, R. M., Drmanic, S., Douville, E. M. J., and Bell, J. C. (1995) *J. Biol. Chem.* **270**, 21524–21531
- Gygi, S. P., Corthals, G. L., Zhang, Y., Rochon, Y., and Aebersold, R. (2000) *Proc. Natl. Acad. Sci. U. S. A.* **97**, 9390–9395
- Lopez, M. F., and Mevlöv, S. (2002) *Circ. Res.* **90**, 380–389